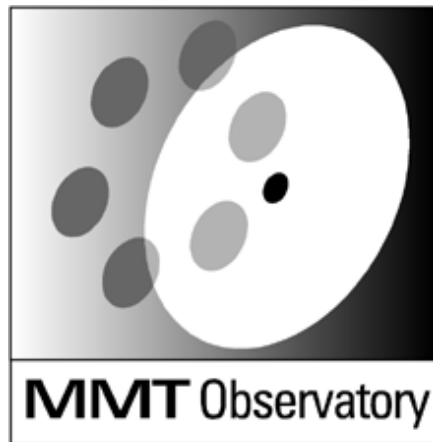


# MMTO Internal Technical Memorandum #02-2



Smithsonian Institution &  
The University of Arizona®

## MMT Mount Control System Operation and Performance

D. Clark

November 2002

**MMT Mount Control System  
Operation and Performance**

**Dusty Clark  
November 20, 2002**

**Version 1.0**

## Introduction

The MMT mount control system is based on realtime control software running VxWorks on a VME processor. It processes all the required functions (i.e. precession/nutation, pointing corrections, offsets, LST acquisition, and others) for acquiring sky positions for stellar and non-stellar objects by controlling the position of the telescope azimuth, elevation and instrument rotator positions.

All axes of the telescope are fully interlocked to a safety control system and is constantly monitored and controlled by the mount control software. For interfacing to the telescope operator, Ethernet communications to a GUI are implemented to a Linux-based operators' computer.

This paper will describe the major components of the control system, their operation, and the achieved performance to date.

## Major System Components

Refer to the block diagram (Figure 1) for an overview of the interconnection between the components described below.

### VME Computer

The heart of the system is the VME control computer. It contains the CPU and all the required I/O boards for handling the system interfaces. The CPU is a Motorola MVME-167, and the I/O support is handled by a collection of IP-Carrier cards that house various Industry-Pack modules and an Acromag 9331 analog I/O card that collects low-priority analog signals in the system (such as building error, elevation motor currents, etc.).

The IP-carrier boards hold the Greenspring IP-Digital24 boards for connection to the interlock system, the IP-Digital48 boards for absolute encoder data acquisition, and IP-Servo boards for LM-628 based control of the telescope motor servo loops.

### IP-Carrier Boards

Several Greensprings IP-Carrier boards are installed in the VME chassis. Each carrier can handle four IndustryPack modules. For the interlock system, these are IP-Digital24 units. They provide digital i/o 24 bits wide, with each bit programmable as input or output. For the absolute encoder interface, they are IP-Digital48 units. Thirty-two bits for each unit is used on the input bits from the absolute encoder system. For driving the velocity loops of the azimuth, elevation, and rotator axes, they are IP-Servo units. Each IP-Servo has a pair of National Semiconductor LM628 servo controllers, which require an incremental encoder feedback and output an analog  $\pm 5V$  motor control signals at 12-bit resolution.

### Mount Interface Chassis

All of the telescope servo loop control signals to and from the VME computer pass through this chassis. It provides a central location for test and troubleshooting and galvanic isolation between the computer and all of the other system hardware. The computer grounds are *never* connected to any other ground to provide the highest possible lightning and noise immunity.

In the chassis, only two types of in-house designed cards are mounted: one handles the i/o for an IP-Servo (4 are required to run the telescope), and the other is an opto-isolator card for passing the absolute encoder signals to the IP-Digital48. Several slots are wired, but none currently used, for housing an interface card for a pair of IP-Quadrature boards (each IP-Quadrature handles 4 incremental encoder counting channels). These boards provide all the necessary isolation for handling the servo amplifier commands to the amplifiers, incremental encoder inputs, and absolute encoder feedback.

### Safety Interlock System

The safety interlocks for the telescope consists of many series-connected limit switches and buttons for determining if a particular axis is ready to run. If this is the case, the mount control software can then energize the appropriate contactor or relay to turn on amplifiers, release brakes, etc.

In addition, an emergency-stop chain is provided to provide an immediate shutdown of all telescope axes, shutters, and brakes in case of an emergency. Emergency-stop buttons are located around the perimeter of the telescope chamber and in the control room at the operators and observer's consoles. Recovery from an emergency-stop condition requires a manual, not computer-controlled, reset.

The condition of each limit switch or other input to the axis-ready chains is tied into the mount control software via a large array of G5 input modules connected to IP-Digital24 units. Output from the computer is likewise handled by an array of G5 output modules so the computer is again isolated from the building-wide interlock wiring.

### Analog I/O Chassis

To handle low-priority analog signals that need to be monitored, a separate isolation chassis is connected to the VME chassis' Acromag 9331 data-acquisition board. This chassis holds a 16-slot industry-standard 5B module rack that contains the module in each slot appropriate to the signal being monitored (i.e. voltage input, potentiometer input, etc.) In this way, we acquire signals such as the building lvdv error, axial counterweight positions, elevation motor currents.

The chassis also holds an 8-slot G5 rack with 4 inputs and 4 outputs, none of which are used at this time.

### Absolute Encoders

Position feedback to the servos for azimuth and elevation are provided by on-axis Inductosyn-based rotary encoders. The Inductosyns are 1024-pole units, providing 512 electrical output cycles for each shaft revolution. Each Inductosyn is connected to a geared resolver to provide cyclical resolution of the Inductosyn electrical cycle. The combination of the resolver value (16-bits) and the Inductosyn readout (also 16-bits) value are meshed in software to provide a 25-bit absolute position to the mount control software. All of the analog signal-conditioning hardware for the encoders is housed in a steel chassis next to each encoder, and digital output values are passed to the computer via optical isolation in the mount interface chassis.

### Incremental Encoders

Incremental encoders are used for velocity-loop feedback to the IP-Servo units. For azimuth, this signal is provided by a single Heidenhain RON905 encoder mounted on one of the azimuth motors. The RON905 has 36,000 cycles/rev of output, which is in turn interpolated by 5X by a Heidenhain EXE602E interpolator. The resultant A,B, and index quadrature counting pulses are then fed back through the mount interface isolation to the LM628 on the IP-Servo.

The elevation axis has gone through a number of iterations since commissioning. The original configuration had two LM628 loops, one for each elevation motor. The velocity-loop feedback came from RON905s mounted on the motor shafts, interpolated 25X by Heidenhain EXE702 units. This was not particularly successful, as we discovered that torque-sharing between the two motor loops was not developing; instead, one loop would "win" and end up doing all the work, with the other idling and not providing any drive stiffness. We then changed to a single feedback from one motor encoder driving one LM628, which in turn had its' output signal applied to both elevation motor drive amplifiers. This was somewhat better and more stable for servo tuning. The latest revision to this encoder feedback configuration is the addition of Heidenhain linear encoder tapes to the elevation drive arcs. One side was aligned and applied to the

EXE702, giving the slightly-lower feedback resolution to the same single LM628 – double motor drive combination. This has given the best performance to date.

The rotator axis uses two read heads on a single Heidenhain linear encoder tape wrapped around the outside of the rotator bearing housing for incremental counting inputs and absolute positioning. Absolute position is acquired by traversing two contiguous index marks, which are placed on the tape a varying distance apart that is unique for every pair of marks. The incremental pulses are used by an LM628 loop to control the motor drive amplifiers.

### Motor Drive Amplifiers

The mount interface outputs the isolated control signals from the LM628 controllers to amplifiers for the azimuth, elevation, and rotator axes. The azimuth axis uses four linear power amplifiers, developed and built in-house in 2000 to replace the aging, unreliable CSR amplifier design. The original chassis were reused and a new transformer, rectifier, drive card, and output transistor stage were installed. Each amplifier can output  $\pm 24\text{V}$  at 18A, continuous.

For elevation and rotator axes, Copley Controls PWM amplifiers are used. All are Model 220 units, with a single master unit used in each of the four rotator motors, and a master/slave combination used for the elevation motors. They use a 60VDC unregulated bus, and a single master can output up to 18A peak, 12A continuous at  $\pm 75\text{V}$ . Adding a slave unit doubles the output current, as required for the elevation drives.

### Motor Drives

All motor drives utilize permanent-magnet DC brush motors. The azimuth units are the original units installed circa 1976: Inland model TT-10039A with an integral tachometer. Four are installed around the telescope yoke and drive a common bull gear through individual 100:1 gearboxes.

The rotator uses a pair of gearboxes, each with two Kollmorgen QT-6207 motors installed to drive a common bull gear on the outside of the rotator bearing. Both motors connect to a common intermediate gear that is in turn connected to a pinion gear that drives the bull gear, for a resultant mechanical advantage of 65:1.

The elevation uses a friction drive with a 27.5:1 mechanical advantage on each side of the primary mirror cell. The drive motor units house the RON905 encoder, an electrically-released brake, and a Kollmorgen QT-13701A motor.

### **Servo System Operation**

Block diagrams of the the elevation, azimuth, and rotator servo axes are shown in figures 2,3, and 4, respectively. All of the MMT servo loops use a dual-loop PID servo architecture, with an inner velocity loop closed with an LM628 controller utilizing incremental encoder pulse feedback, and an outer position loop closed with the VME CPU with the on-axis absolute encoders used for position feedback. All of the servo amplifiers run in current-source (torque) mode, with the gains noted on the block diagram.

The inner-loop LM628s for the elevation axis used the motor-shaft encoders in the early stages of telescope operation, with both units available on an IP-Servo card commanding the two elevation drive motors. This led to a number of performance issues, and the system has since evolved to the one shown on Figure 3, where the existing motor encoders are unused and the original 25X interpolators are now connected to the tape encoder read head outputs. One of the two LM628s is used to drive the servo, while the other is used for tape encoder position acquisition. The encoder tape is a Heidenhain LIDA105C, with a basic counting mark pitch of 40 microns and quasi-absolute index marks (as used on the rotator axis). The LM628 accepts a velocity demand from the VME CPU at 100Hz, while internally running its PID loop on the incremental encoder feedback at 3096Hz. Refer to the included LM628 documentation for more detailed information on its operation.

The azimuth axis also runs an outer position loop at 100Hz, with the LM628 loop closed on a single motor shaft, of the four in the drive system. Since the azimuth axis is gear-driven, as opposed to the elevation, which is a friction drive, an anti-backlash constant torque of alternating sign is applied to each of the motor amplifiers. This servo architecture is essentially unchanged since the telescope commissioning. A known problem with this drive system is the backlash in the geartrain and the lack of rigidity in the gearbox mounting system. This system is shown in Figure 3.

The rotator axis originally used a set of 4 LM628s, each closed around a motor shaft encoder and an outer loop closed around the tape encoder, with absolute positions acquired at startup by measuring the unique distance between index marks on the tape. This unfortunately failed due to the exposure of the motor encoders to disturbance and rough handling during gearbox installation. All of the motor encoders failed and have since been removed. In the current configuration, shown in Figure 4, an LM628 loop is closed around one tape head, with the other tape head applied to the alternate LM628 on the IP-Servo card. This arrangement gives access to both counting pulses and index marks for the outer loop to acquire the absolute position and run the outer position loop.

All of the servo axes run the same outer loop PID algorithm (Figure 5). This algorithm takes the current demanded position, reads the encoders, and calculates the position and velocity error. Based on the absolute magnitude of the position and velocity error, the servo loop applies one of several output calculations to arrive at a velocity demand to the inner loop (this is a switch-mode PID). A velocity feed-forward term is always added to the output, and velocity and jerk clipping is applied before the output value is written to the LM628. The output modes take on these characteristics:

- 1. Velocity error and Position error both over Verr and Perr limit values:**  
The servo loop calculates an output value equal to a gain factor times the square root of the position error. This is referred to (and flagged as) Gross mode in the servo.
- 2. Velocity error greater than Verr and Position error less than Perr limit value:**  
The servo loop then moves into Rough mode, with the standard Proportional gain term calculated and an additional Derivative term also added to the output.
- 3. Both velocity error and position error less than Verr and Perr limit values:**  
At this point, the axis has gotten close to the target position and velocity, so the Proportional term and Derivative terms are summed with an Integral term to achieve a full PID with velocity feed-forward. In the software, this is called Tight mode.

For testing, tuning, and measuring servo performance, a GUI was developed that gives access to the servo gain term values for both loops and another for graphing system outputs such as velocity and position error in realtime. A typical graph is shown in Figure 6.

Initial system tuning (i.e. adjustment of the LM628 PID gain terms and the outer loop mode gains and switch point values) make use of these tools to arrive at a stable and well-behaved servo loop. For characterization of the motor position loop, we use an open-loop test that requires a Dynamic Signal Analyzer and a DSP board. In this test, we excite the motor/amplifier/encoder loop with a swept-sine signal that typically varies from 0.2Hz to 20Hz, with the encoder output converted to an analog signal proportional to the encoder displacement. In special cases, we have the capability to convert the absolute encoder's parallel digital format to incremental pulses and apply those to the conversion electronics. The conversion is done with a DSP board, an Advanced Realtime Control Systems Lightning DSP board, running test software compiled with Matlab Simulink and Real-time Workshop targeting the Lightning DSP unit. The combination of the ARCS board and Simulink/Real-time Workshop gives a powerful diagnostic tool for measuring and analyzing test results.

## Servo Testing and System Characteristics

Much testing has been done to characterize the open-loop behavior of the azimuth and elevation axes of the telescope. Little has been done on the rotator as it performs well and appears to exhibit no undesirable operational modes.

For elevation, open-loop tests as shown in Figure 7 have been done quite extensively. Most of the effort has concentrated on understanding and locating the cause of a low-frequency resonance in the drivetrain not predicted by the mechanical designer's FEA results. A plot of the results from one of these tests is shown in Figures 9 and 10. Figure 9 is the open-loop transfer function to the motor shaft, while Figure 10 is the same test but with the feedback variable coming from the tape head encoder. The relatively low-frequency peak at 2Hz is not predicted by FEA modeling and is currently not well understood. It was suspected that this was caused by a compliant mode in the elevation motor mounting and preload flexure system. The flexures have since been replaced with much stiffer flexures, with no corresponding increase in the resonant frequency. Rigid-body modes measured with an accelerometer show an improvement in the motor housing modes of a magnitude predicted by basic stiffness calculations of the flexures.

More testing has since been done using an accelerometer to try to locate a resonant point or component on the telescope structure, with inconclusive results.

Azimuth has had a few open-loop tests, which mainly serve to confirm the results obtained in the 1980s that the azimuth drivetrain exhibits a 3.3Hz resonant mode that is due to the compliance of the geartrain and the gearbox mounting system stiffness. MMTO currently has a design proposal to remove the gearboxes and replace them with a much stiffer mounting system, along with a single pinion gear attached rigidly to the motor shaft. This plan would re-use the existing motors at a considerable cost savings in this project.

Closed-loop tests (set up as shown in Figure 8) result in output plots that show the limits of the PID loops to deal with the onset of oscillation in the resonant structural modes of the telescope. This is perhaps the greatest impediment to improving the drive stiffness in elevation. Servo gains high enough for good disturbance (i.e. wind) rejection push the servo gains beyond stability due to the rapid change in the system gain and phase characteristics. Plots of the open and closed-loop behavior of the azimuth and elevation axes acquired with the HP DSA are attached as Figures 9 through 13.

## Performance Limitations

The current servos have a few serious shortcomings that limit the scientific performance of the telescope. These problems are:

1. Low-frequency structural modes in the elevation axis that limit the range of stable gain values to levels too low for good wind disturbance rejection.
2. The basic inability of PID loops to sense, adjust to, and eliminate resonance, as can be done with more advanced state-observer control algorithms.
3. The fast update rate of the LM628 controller (256 $\mu$ S) leaves the controller with very few encoder counts per sample at sidereal rates, leading to the loss of velocity regulation when tracking, especially when torque disturbances are present.
4. The 12-bit resolution of the LM628 is fairly coarse compared to the encoder system resolutions, so the system can limit-cycle between output codes and never achieve a smoothed output value. Output smoothing is totally dependent on the low-pass filtering provided by the system inertia.
5. Changes to the telescope configuration can lead to servo instability if the servos have not been carefully tuned for every possible combination of instruments, counterweight positions, etc. The default condition is then to use a weaker tuning set that works under most conditions, but is not optimized for the best possible performance for the given telescope configuration.

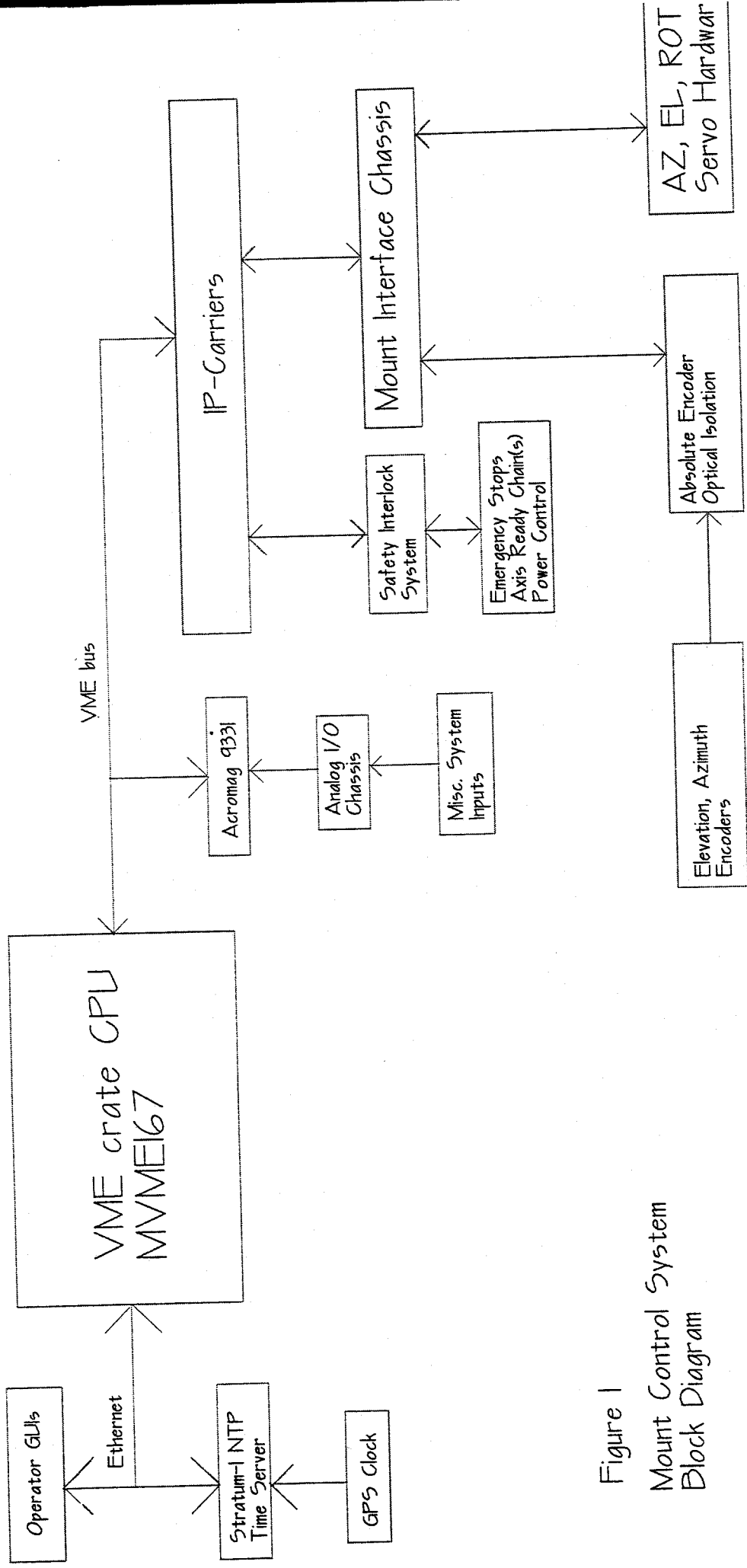


Figure 1  
Mount Control System  
Block Diagram



Figure 2  
MMT Elevation Axis  
Servo Block Diagram

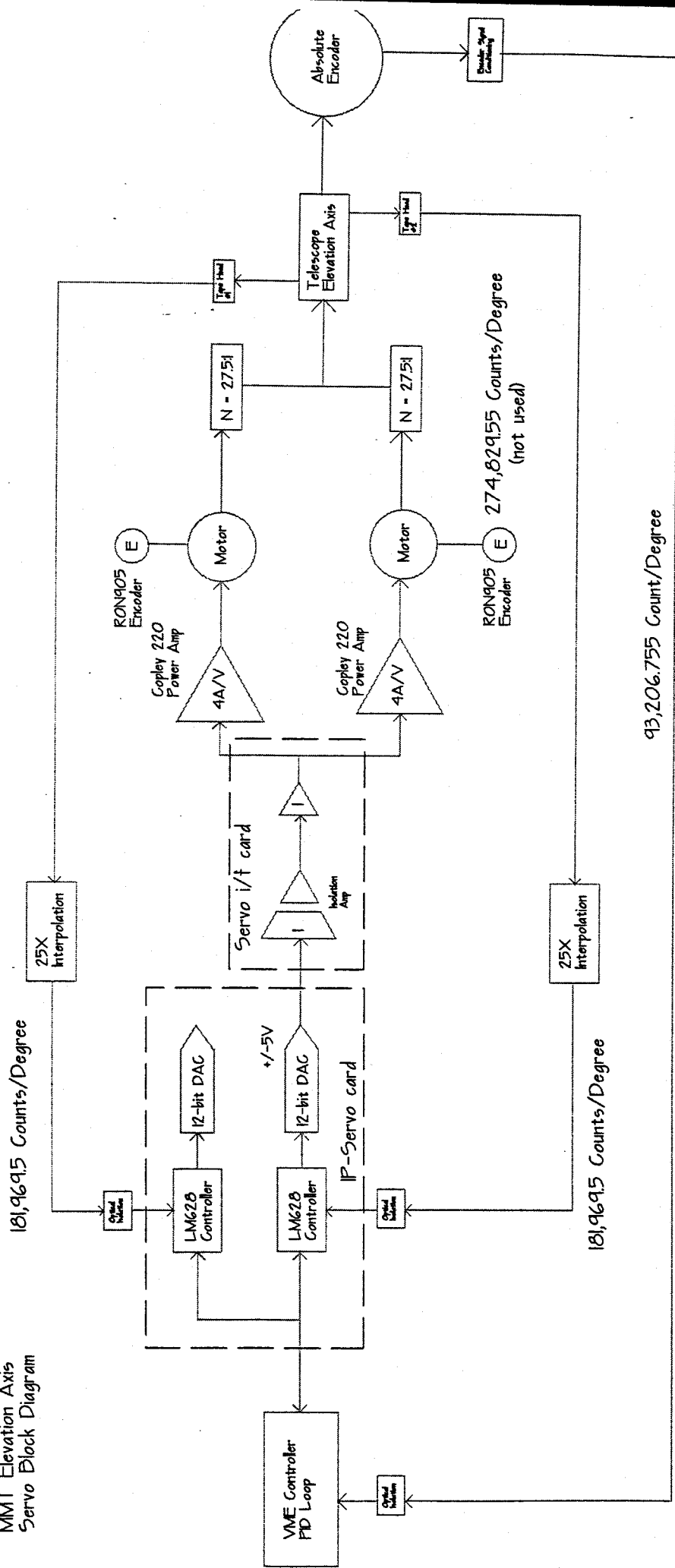
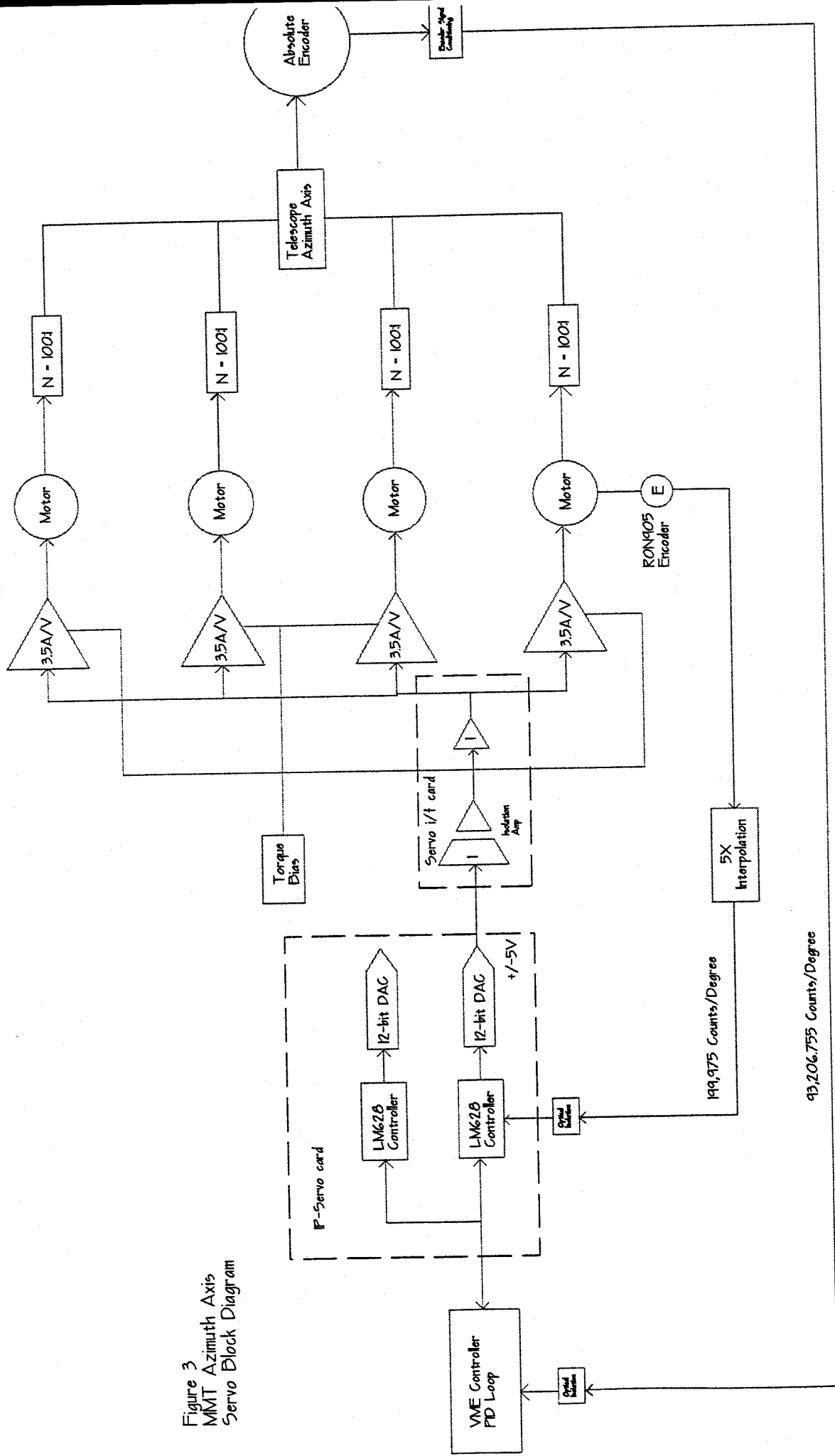


Figure 3  
MMT Azimuth Axis  
Servo Block Diagram



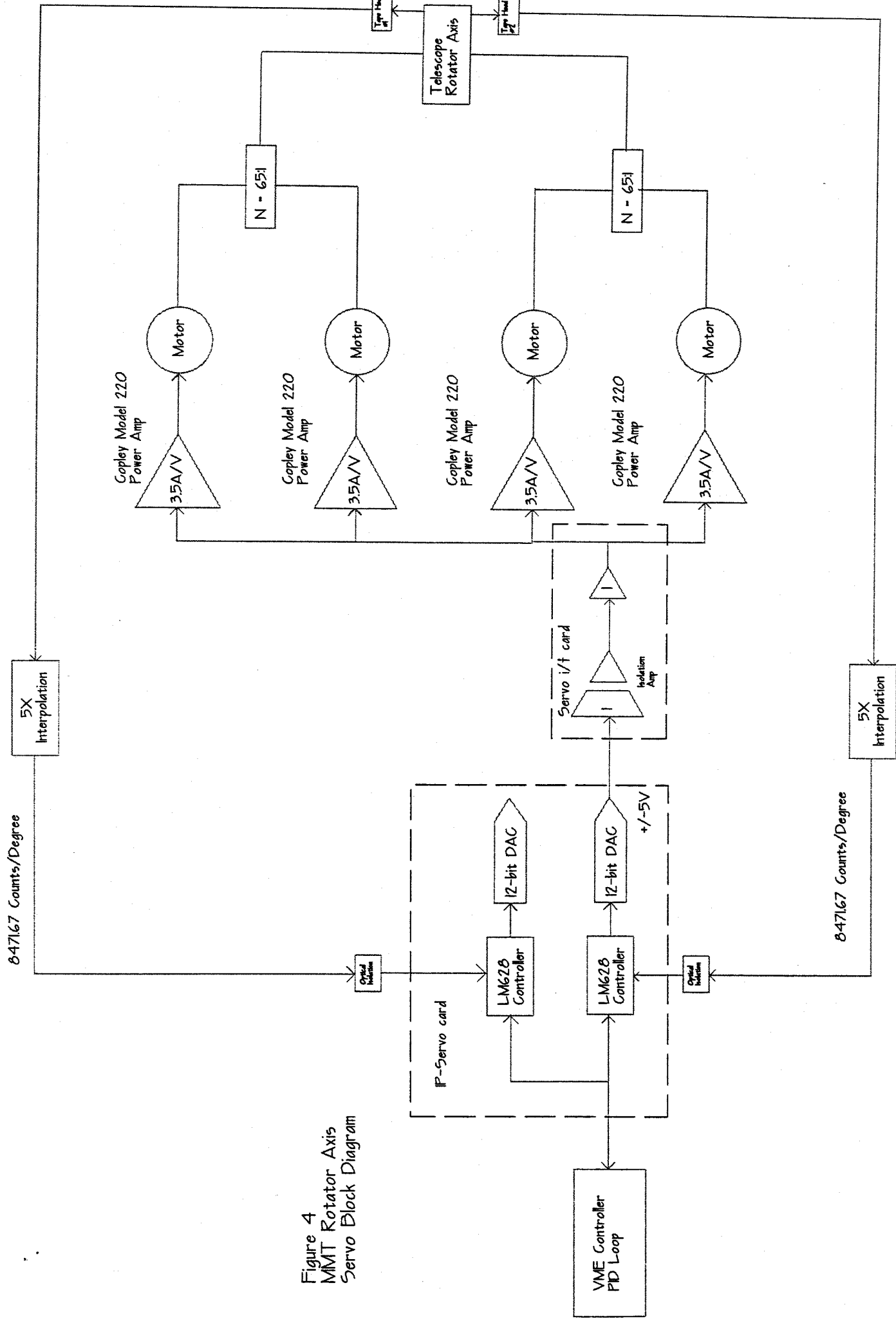


Figure 4  
MMT Rotator Axis  
Servo Block Diagram

Figure 5

# Mount Control Outer Loop Algorithm

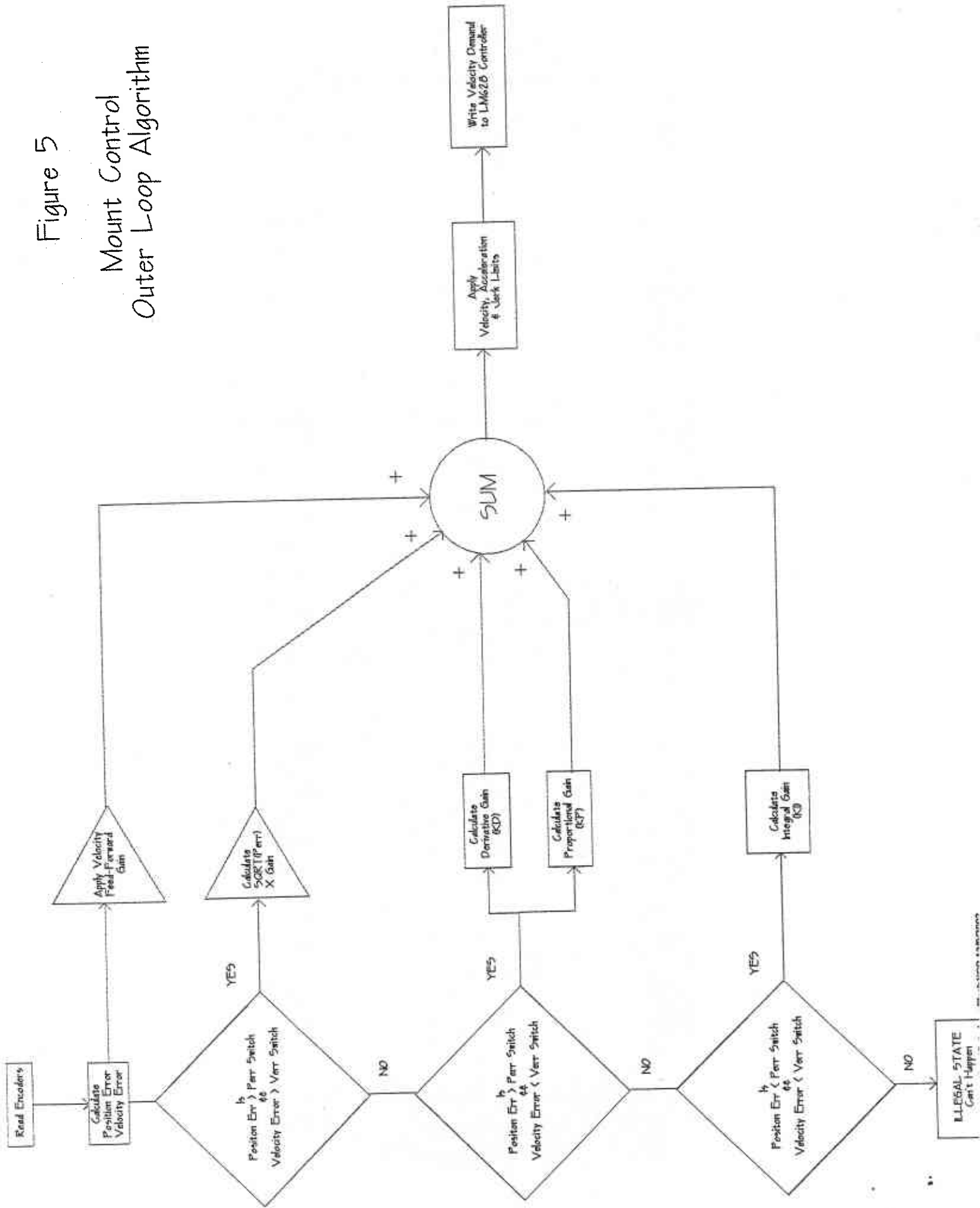


Figure 6a

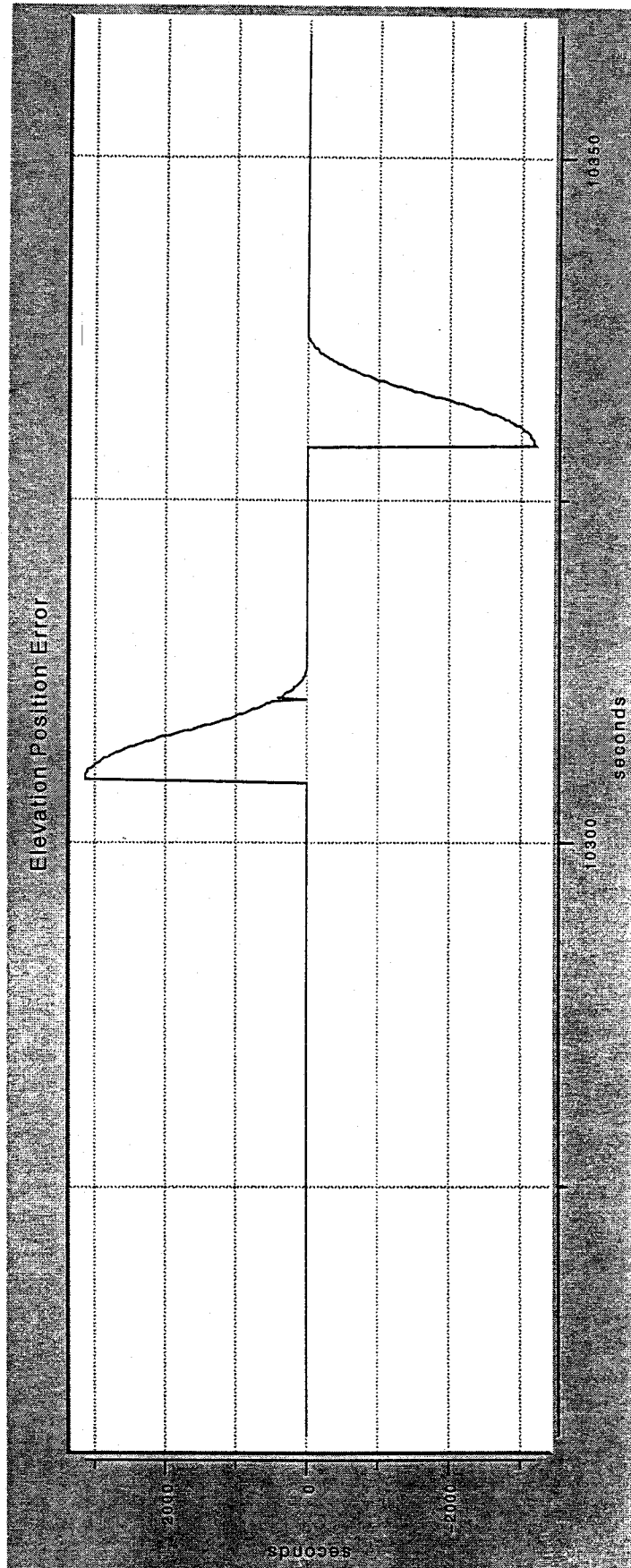


Figure 6b

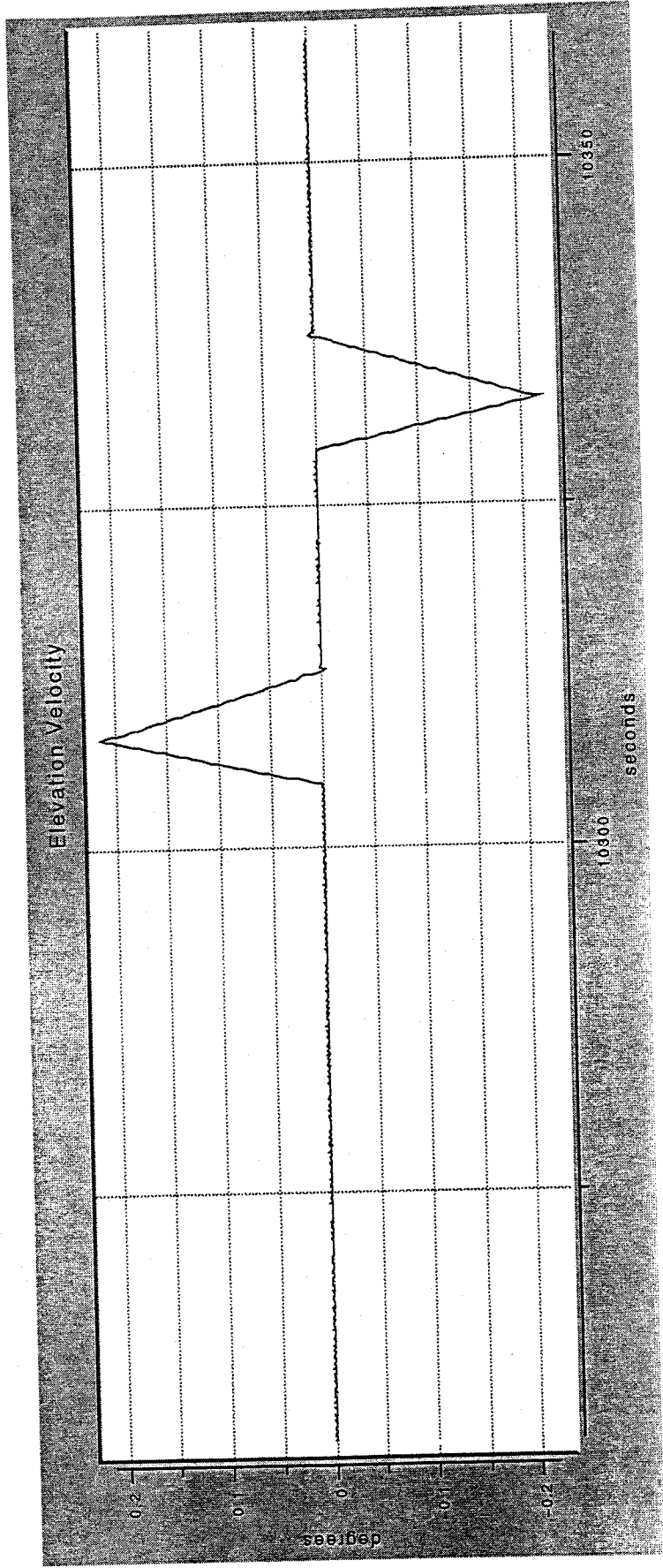
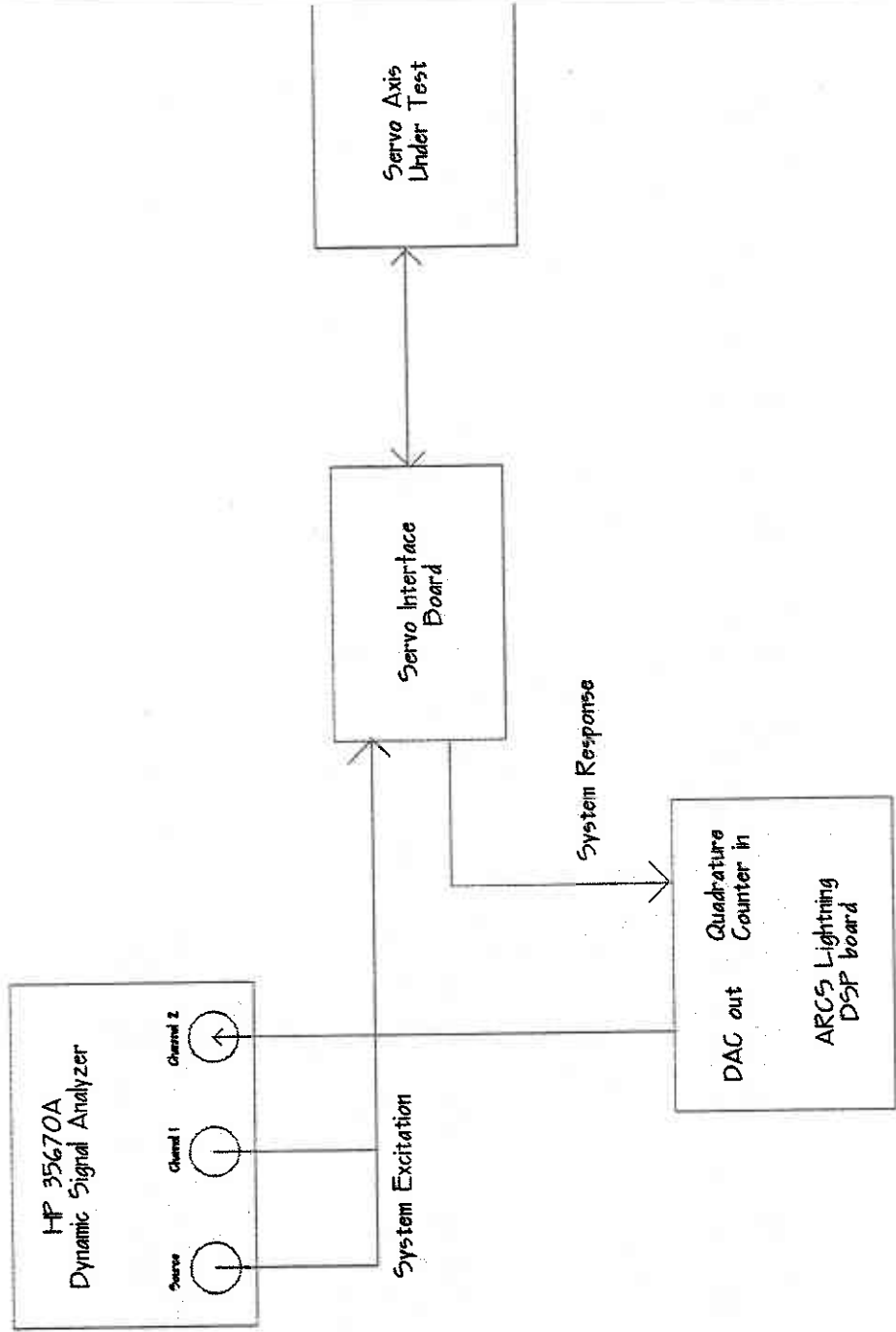


Figure 7  
 Servo Open Loop  
 Transfer Function Test Setup



Quadrature encoder pulses are converted to analog position signals to acquire the transfer function from motor command to motor (or telescope) position

Figure 8  
 Servo Closed Loop  
 Transfer Function Test Setup

A disturbance signal is summed with the control input to the servo loop. The controller output becomes the transfer function output variable.

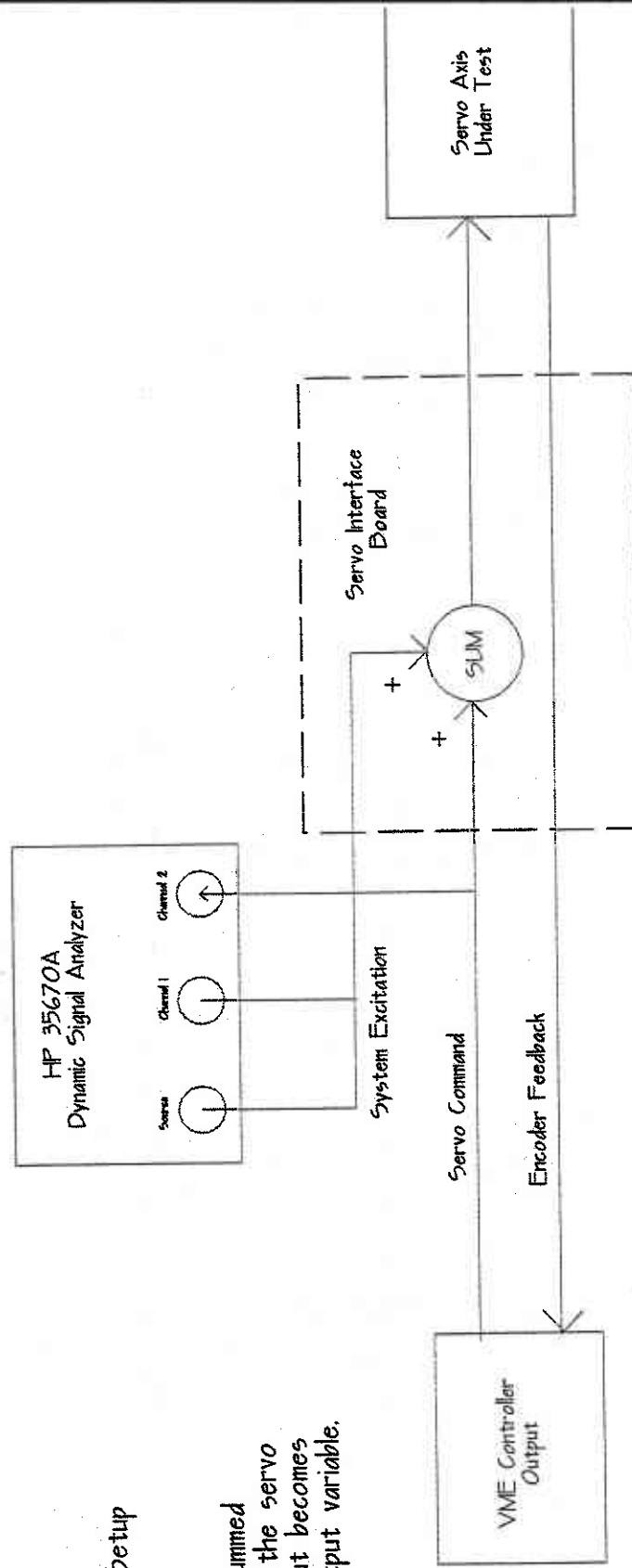




Figure 9

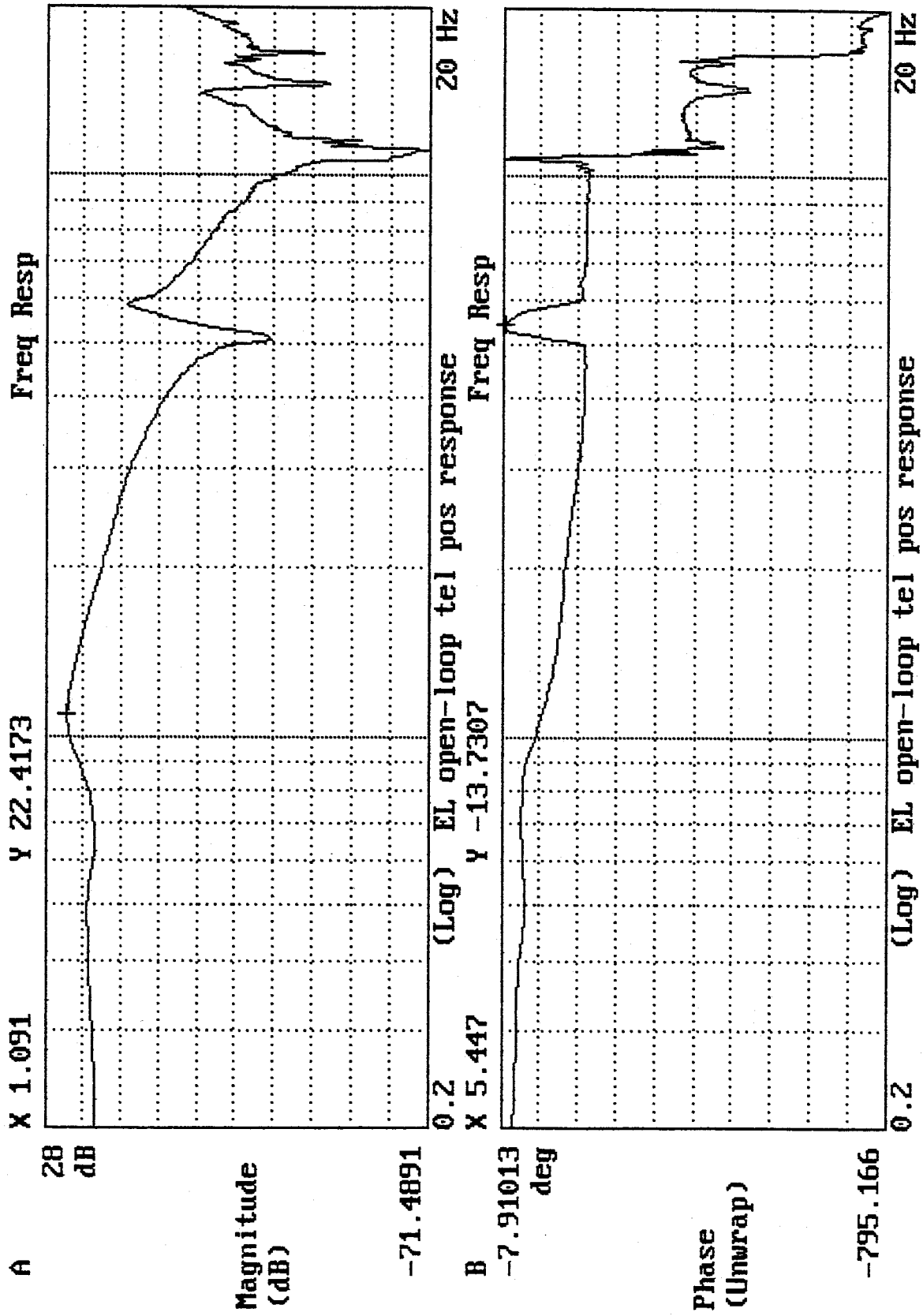


Figure 10

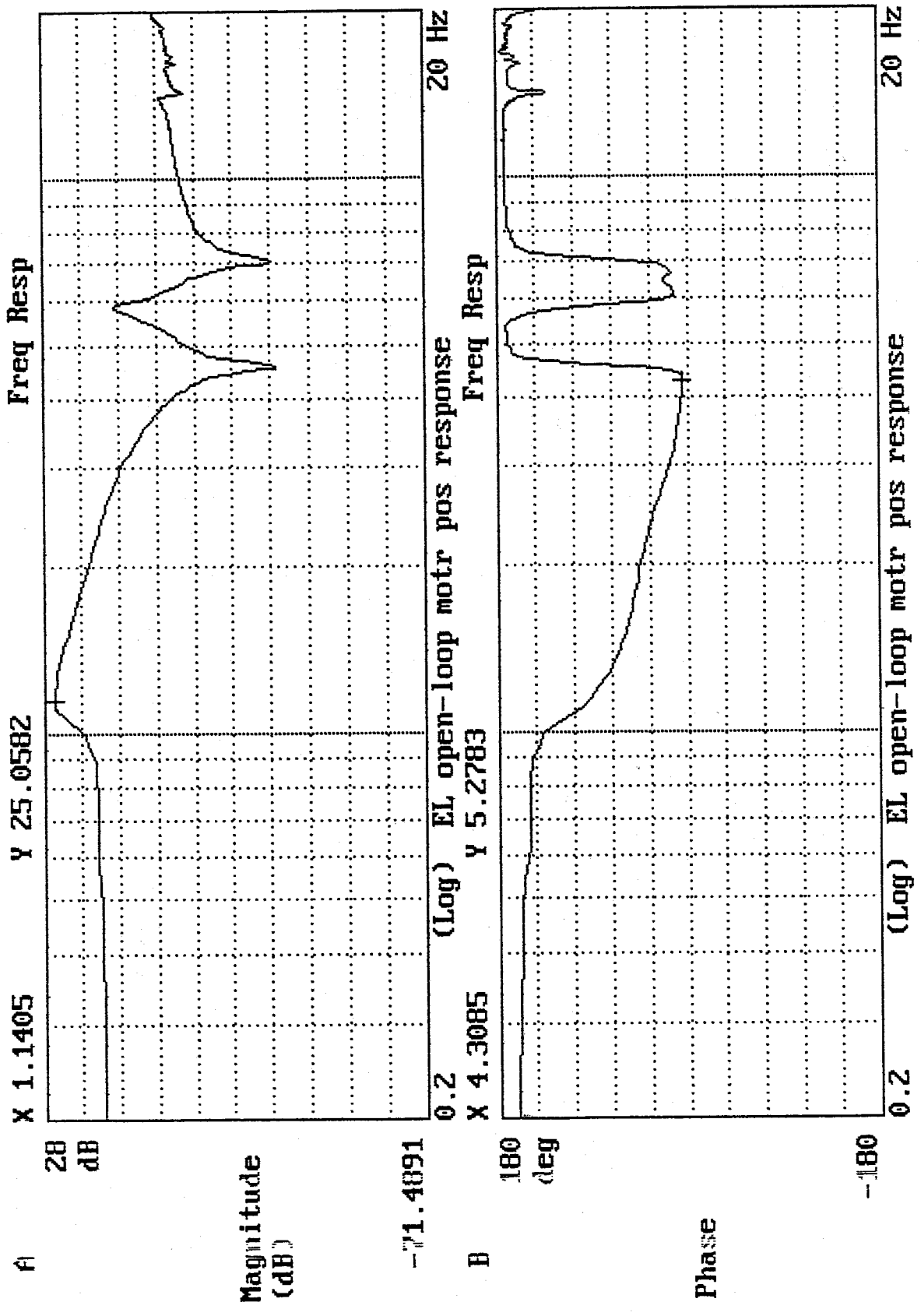


Figure 11

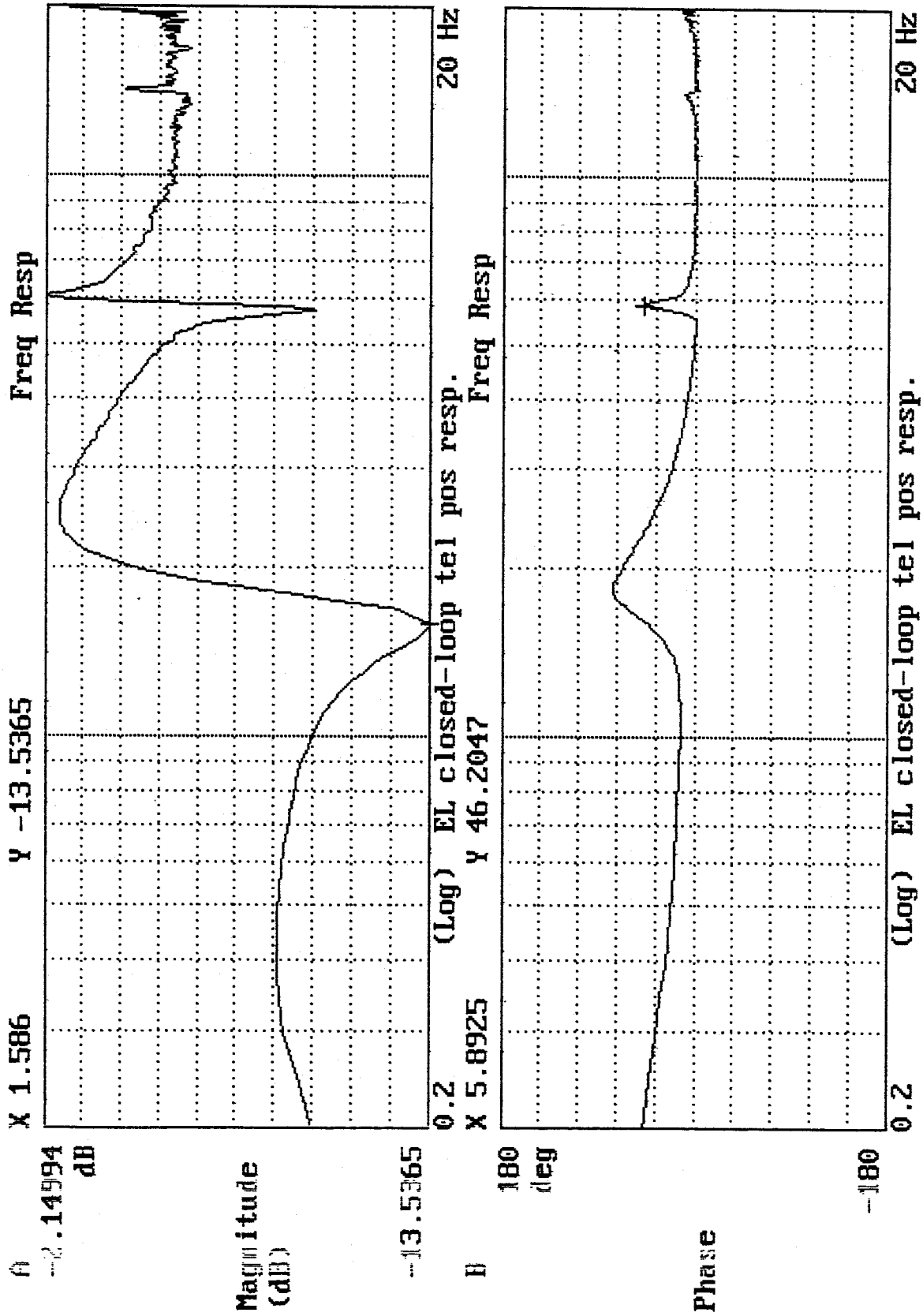


Figure 12

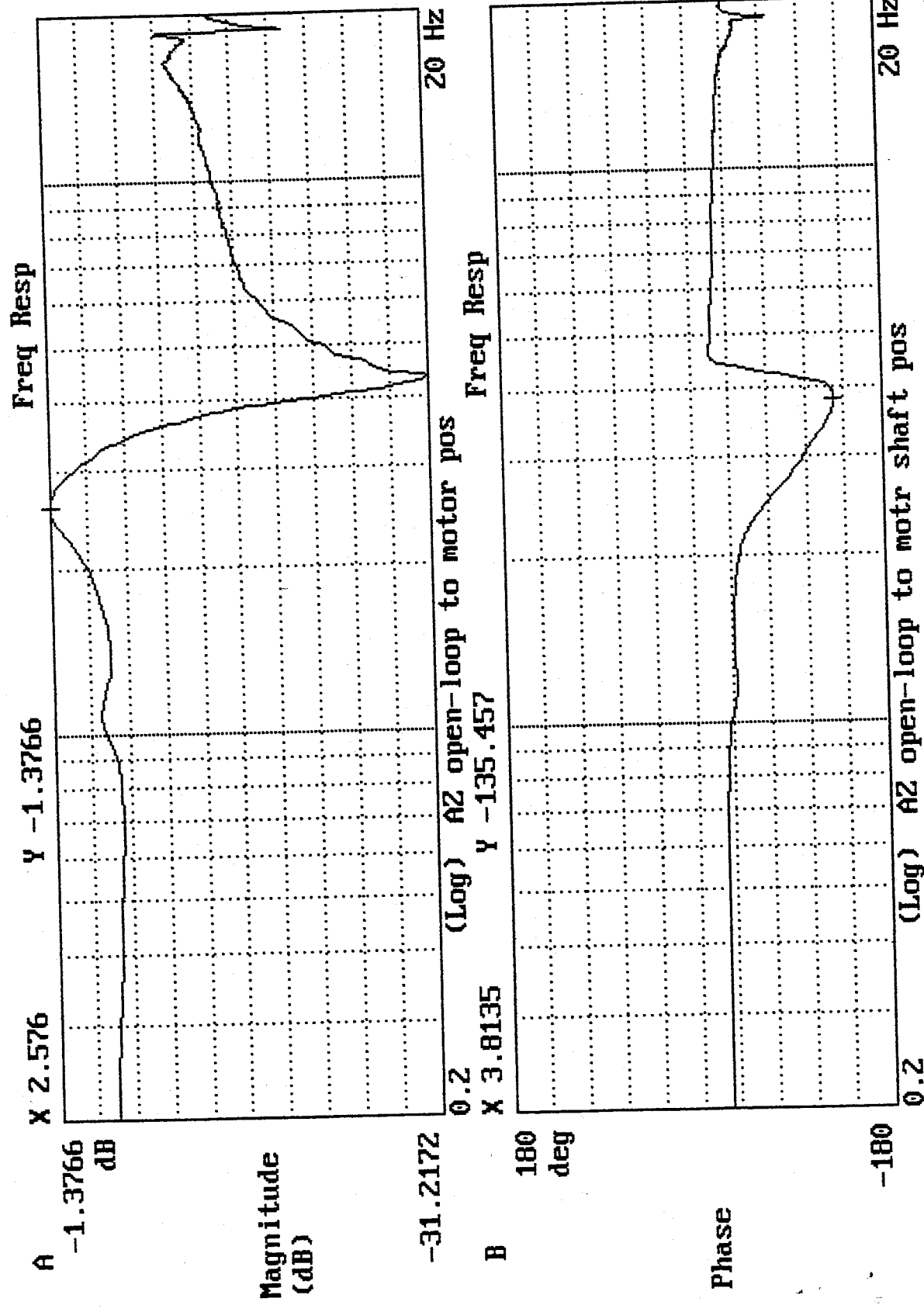


Figure 13

